

OPEN ACCESS

The active muon shield in the SHiP experiment

To cite this article: A. Akmete *et al* 2017 *JINST* **12** P05011

View the [article online](#) for updates and enhancements.

Related content

- [Optimising the Active Muon Shield for the SHiP Experiment at CERN](#)
A Baranov, E Burnaev, D Derkach *et al*.
- [The beam and detector of the NA62 experiment at CERN](#)
E. Cortina Gil, E. Martín Albarrán, E. Minucci *et al*.
- [Upgrade of the ALICE Experiment: Letter Of Intent](#)
B Abelev *et al* and The ALICE Collaboration

Recent citations

- [The magnet of the scattering and neutrino detector for the SHiP experiment at CERN](#)
C. Ahdida *et al*
- [Optimization of the SHiP Spectrometer Tracker geometry using the Bayesian Optimization with Gaussian Processes](#)
Oleg Alenkin *et al*
- [Application of hot isostatic pressing \(HIP\) technology to diffusion bond refractory metals for proton beam targets and absorbers at CERN](#)
Josep Busom Descarrega *et al*

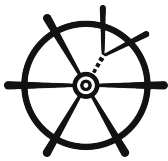


IOP | ebooks™

Bringing you innovative digital publishing with leading voices to create your essential collection of books in STEM research.

Start exploring the collection - download the first chapter of every title for free.

The active muon shield in the SHiP experiment



The SHiP collaboration

A. Akmete,⁴³ A. Alexandrov,¹² A. Anokhina,³⁵ S. Aoki,¹⁶ E. Atkin,³⁴ N. Azorskiy,²⁵
 J.J. Back,⁴⁹ A. Bagulya,²⁸ A. Baranov,³⁶ G.J. Barker,⁴⁹ A. Bay,⁴¹ V. Bayliss,⁴⁶
 G. Bencivenni,¹³ A.Y. Berdnikov,³³ Y.A. Berdnikov,³³ M. Bertani,¹³ C. Betancourt,⁴²
 I. Bezshyiko,⁴² O. Bezshyyko,⁵⁰ D. Bick,⁷ S. Bieschke,⁷ A. Blanco,²⁴ J. Boehm,⁴⁶
 M. Bogomilov,¹ K. Bondarenko,⁵⁰ W.M. Bonivento,¹¹ A. Boyarsky,⁵⁰ R. Brenner,³⁸ D. Breton,⁴
 R. Brundler,⁴² M. Bruschi,¹⁰ V. Büscher,⁸ A. Buonauro,^{12,a} S. Buontempo,¹² S. Cadeddu,¹¹
 A. Calcaterra,¹³ M. Campanelli,⁴⁸ J. Chauveau,⁵ A. Chepurinov,³⁵ M. Chernyavsky,²⁸
 K.-Y. Choi,²¹ A. Chumakov,² P. Ciambone,¹³ G.M. Dallavalle,¹⁰ N. D'Ambrosio,^{12,14}
 G. D'Appollonio,^{11,b} G. De Lellis,^{12,d} A. De Roeck,³⁹ M. De Serio,^{9,c} L. Dedenko,³⁵ A. Di
 Crescenzo,^{12,a} N. Di Marco,¹⁴ C. Dib,² H. Dijkstra,³⁹ V. Dmitrenko,³⁴ D. Domenici,¹³
 S. Donskov,³¹ A. Dubreuil,⁴⁰ J. Ebert,⁷ T. Enik,²⁵ A. Etenko,²⁹ F. Fabbri,¹⁰ L. Fabbri,^{10,d}
 O. Fedin,³² G. Fedorova,³⁵ G. Felici,¹³ M. Ferro-Luzzi,³⁹ R.A. Fini,⁹ P. Fonte,²⁴ C. Franco,²⁴
 T. Fukuda,¹⁷ G. Galati,^{12,d} G. Gavrillov,³¹ S. Gerlach,⁶ L. Golinka-Bezshyyko,⁵⁰ D. Golubkov,²⁶
 A. Golutvin,⁴⁷ D. Gorbunov,²⁷ S. Gorbunov,²⁸ V. Gorkavenko,⁵⁰ Y. Gornushkin,²⁵
 M. Gorshenkov,³⁰ V. Grachev,³⁴ E. Graverini,⁴² V. Grichine,²⁸ A. M. Guler,⁴³ Yu. Guz,³¹
 C. Hagner,⁷ H. Hakobyan,² E. van Herwijnen,³⁹ A. Hollnagel,⁷ B. Hosseini,¹¹ M. Hushchyn,³⁶
 G. Iaselli,^{9,c} A. Iuliano,^{12,a} R. Jacobsson,³⁹ M. Jonker,³⁹ I. Kadenko,⁵⁰ C. Kamiscioglu,⁴⁴
 M. Kamiscioglu,⁴³ M. Khabibullin,²⁷ G. Khaustov,³¹ A. Khotyantsev,²⁷ S.H. Kim,²⁰ V. Kim,^{32,33}
 Y.G. Kim,²² N. Kitagawa,¹⁷ J.-W. Ko,²³ K. Kodama,¹⁵ A. Kolesnikov,²⁵ D.I. Kolev,¹
 V. Kolosov,³¹ M. Komatsu,¹⁷ N. Konovalova,²⁸ M.A. Korkmaz,⁴³ I. Korol,⁶ I. Korol'ko,²⁶
 A. Korzenev,⁴⁰ S. Kovalenko,² I. Krasilnikova,³⁰ K. Krivova,³⁴ Y. Kudenko,^{27,34} V. Kurochka,²⁷
 E. Kuznetsova,³² H.M. Lacker,⁶ A. Lai,¹¹ G. Lanfranchi,¹³ O. Lantwin,⁴⁷ A. Lauria,^{12,a}
 H. Lebbolo,⁵ K.Y. Lee,²⁰ J.-M. Lévy,⁵ L. Lopes,²⁴ V. Lyubovitskij,² J. Maalmi,⁴ A. Magnan,⁴⁷
 V. Maleev,³² A. Malinin,²⁹ A. Mefodev,²⁷ P. Mermod,⁴⁰ S. Mikado,¹⁸ Yu. Mikhaylov,³¹
 D.A. Milstead,³⁷ O. Mineev,²⁷ A. Montanari,¹⁰ M.C. Montesi,^{12,a} K. Morishima,¹⁷
 S. Movchan,²⁵ N. Naganawa,¹⁷ M. Nakamura,¹⁷ T. Nakano,¹⁷ A. Novikov,³⁴ B. Obinyakov,²⁹
 S. Ogawa,¹⁹ N. Okateva,²⁸ P.H. Owen,⁴² A. Paoloni,¹³ B.D. Park,²⁰ L. Paparella,⁹

A. Pastore,^{9,c} M. Patel,⁴⁷ D. Pereyma,²⁶ D. Petrenko,³⁴ K. Petridis,⁴⁵ D. Podgrudkov,³⁵
V. Poliakov,³¹ N. Polukhina,^{28,34} M. Prokudin,²⁶ A. Prota,^{12,a} A. Rademakers,³⁹ F. Ratnikov,³⁶
T. Rawlings,⁴⁶ M. Razeti,¹¹ F. Redi,⁴⁷ S. Ricciardi,⁴⁶ T. Roganova,³⁵ A. Rogozhnikov,³⁶
H. Rokujo,¹⁷ G. Rosa,¹² T. Rovelli,^{10,d} O. Ruchayskiy,³ T. Ruf,³⁹ V. Samoylenko,³¹ A. Saputi,¹³
O. Sato,¹⁷ E.S. Savchenko,³⁰ W. Schmidt-Parzefall,⁷ N. Serra,⁴² A. Shakin,³⁰
M. Shaposhnikov,⁴¹ P. Shatalov,²⁶ T. Shchedrina,²⁸ L. Shchutska,⁵⁰ V. Shevchenko,²⁹
H. Shibuya,¹⁹ A. Shustov,³⁴ S.B. Silverstein,³⁷ S. Simone,^{9,c} M. Skorokhvatov,^{34,29}
S. Smirnov,³⁴ J.Y. Sohn,²⁰ A. Sokolenko,⁵⁰ N. Starkov,²⁸ B. Storaci,⁴² P. Strolin,^{12,a}
S. Takahashi,¹⁶ I. Timiryasov,⁴¹ V. Tioukov,¹² N. Tosi,¹⁰ D. Treille,³⁹ R. Tsenov,^{1,25} S. Ulin,³⁴
A. Ustyuzhanin,³⁶ Z. Uteshev,³⁴ G. Vankova-Kirilova,¹ F. Vannucci,⁵ P. Venkova,¹
S. Vilchinski,⁵⁰ M. Villa,^{10,d} K. Vlasik,³⁴ A. Volkov,²⁸ R. Voronkov,²⁸ R. Wanke,⁸ J.-K. Woo,²³
M. Wurm,⁸ S. Xella,³ D. Yilmaz,⁴⁴ A.U. Yilmazer,⁴⁴ C.S. Yoon,²⁰ and Yu. Zaytsev²⁶

¹*Faculty of Physics, Sofia University, Sofia, Bulgaria*

²*Universidad Técnica Federico Santa María and Centro Científico Tecnológico de Valparaíso, Valparaíso, Chile*

³*Niels Bohr Institute, University of Copenhagen, Copenhagen, Denmark*

⁴*LAL, Université Paris-Sud 11, CNRS/IN2P3, Orsay, France*

⁵*LPNHE, Université Pierre et Marie Curie, Université Paris Diderot, CNRS/IN2P3, Paris, France*

⁶*Humboldt-Universität zu Berlin, Berlin, Germany*

⁷*Universität Hamburg, Hamburg, Germany*

⁸*Johannes Gutenberg Universität Mainz, Mainz, Germany*

⁹*Sezione INFN di Bari, Bari, Italy*

¹⁰*Sezione INFN di Bologna, Bologna, Italy*

¹¹*Sezione INFN di Cagliari, Cagliari, Italy*

¹²*Sezione INFN di Napoli, Napoli, Italy*

¹³*Laboratori Nazionali dell'INFN di Frascati, Frascati, Italy*

¹⁴*Laboratori Nazionali dell'INFN di Gran Sasso, L'Aquila, Italy*

¹⁵*Aichi University of Education, Kariya, Japan*

¹⁶*Kobe University, Kobe, Japan*

¹⁷*Nagoya University, Nagoya, Japan*

¹⁸*College of Industrial Technology, Nihon University, Narashino, Japan*

¹⁹*Toho University, Funabashi, Chiba, Japan*

²⁰*Gyeongsang National University, Jinju, Korea*

²¹*Chonnam National University,^e Gwangju, Korea*

²²*Gwangju National University of Education,^e Gwangju, Korea*

²³*Jeju National University,^e Jeju, Korea*

²⁴*LIP, Universidade de Coimbra, Coimbra, Portugal*

²⁵*Joint Institute of Nuclear Research (JINR), Dubna, Russia*

²⁶*Institute of Theoretical and Experimental Physics (ITEP) NRC 'Kurchatov Institute', Moscow, Russia*

²⁷*Institute for Nuclear Research of the Russian Academy of Sciences (INR RAS), Moscow, Russia*

²⁸*P.N. Lebedev Physical Institute (LPI), Moscow, Russia*

²⁹*National Research Centre 'Kurchatov Institute', Moscow, Russia*

³⁰*National University of Science and Technology "MISIS",^f Moscow, Russia*

- ³¹*Institute for High Energy Physics (IHEP) NRC ‘Kurchatov Institute’, Protvino, Russia*
³²*Petersburg Nuclear Physics Institute (PNPI) NRC ‘Kurchatov Institute’, Gatchina, Russia*
³³*St. Petersburg Polytechnic University (SPbPU),^g St. Petersburg, Russia*
³⁴*National Research Nuclear University (MEPhI), Moscow, Russia*
³⁵*Skobeltsyn Institute of Nuclear Physics of Moscow State University (SINP MSU), Moscow, Russia*
³⁶*Yandex School of Data Analysis, Moscow, Russia*
³⁷*Stockholm University, Stockholm, Sweden*
³⁸*Uppsala University, Uppsala, Sweden*
³⁹*European Organization for Nuclear Research (CERN), Geneva, Switzerland*
⁴⁰*University of Geneva, Geneva, Switzerland*
⁴¹*École Polytechnique Fédérale de Lausanne (EPFL), Lausanne, Switzerland*
⁴²*Physik-Institut, Universität Zürich, Zürich, Switzerland*
⁴³*Middle East Technical University (METU), Ankara, Turkey*
⁴⁴*Ankara University, Ankara, Turkey*
⁴⁵*H.H. Wills Physics Laboratory, University of Bristol, Bristol, United Kingdom*
⁴⁶*STFC Rutherford Appleton Laboratory, Didcot, United Kingdom*
⁴⁷*Imperial College London, London, United Kingdom*
⁴⁸*University College London, London, United Kingdom*
⁴⁹*University of Warwick, Warwick, United Kingdom*
⁵⁰*Taras Shevchenko National University of Kyiv, Kyiv, Ukraine*
^a*Università di Bari, Bari, Italy*
^b*Università di Bologna, Bologna, Italy*
^c*Università di Cagliari, Cagliari, Italy*
^d*Università di Napoli “Federico II”, Napoli, Italy*
^e*Associated to Gyeongsang National University, Jinju, Korea*
^f*Associated to P.N. Lebedev Physical Institute (LPI), Moscow, Russia*
^g*Associated to Petersburg Nuclear Physics Institute (PNPI), Gatchina, Russia*

E-mail: Hans.Dijkstra@cern.ch

ABSTRACT: The SHiP experiment is designed to search for very weakly interacting particles beyond the Standard Model which are produced in a 400 GeV/c proton beam dump at the CERN SPS. An essential task for the experiment is to keep the Standard Model background level to less than 0.1 event after 2×10^{20} protons on target. In the beam dump, around 10^{11} muons will be produced per second. The muon rate in the spectrometer has to be reduced by at least four orders of magnitude to avoid muon-induced combinatorial background. A novel active muon shield is used to magnetically deflect the muons out of the acceptance of the spectrometer. This paper describes the basic principle of such a shield, its optimization and its performance.

KEYWORDS: Detector design and construction technologies and materials; Performance of High Energy Physics Detectors

Contents

1	Introduction	1
2	The basic principle of magnet based muon shielding	3
3	Simulations and optimization	3
4	Active muon shield performance	4
5	Discussion and outlook	7

1 Introduction

The SHiP experiment [1] is a new general purpose fixed target facility proposed at the CERN SPS accelerator to search for new physics in the largely unexplored domain of very weakly interacting particles with masses below $O(10)\text{GeV}/c^2$ and $c\tau$ of kilometers [2]. The facility is designed to maximize the production of charm and beauty mesons, while providing the cleanest possible environment. The 400 GeV/c proton beam extracted from the SPS will be dumped into a molybdenum-tungsten target, with the aim of accumulating 2×10^{20} protons on target (POT) during five years of operation. The charm production at SHiP exceeds that of any existing or presently planned facility.

For radiation protection, a 5 m thick iron shield is placed behind the target to absorb hadrons. The SPS will deliver 4×10^{13} POT during a one second long spill, which produces on the order of 10^{11} muons/s mainly from the decay of π , K, ρ , ω and charmed mesons. These muons would give rise to a serious background for many hidden particle searches, and hence their flux has to be reduced by at least four orders of magnitude. The SHiP experiment will use of a series of magnets to deflect the muons out of the acceptance of the spectrometer. Any hidden sector particle originating from charm or beauty meson decay will be produced with a significant transverse momentum with respect to the beam axis.¹ In order to maximize acceptance, the detector therefore should be placed as close as possible to the target, and hence the muon shield should be as short as possible. Behind the muon shield a dedicated detector will probe a variety of models with long lived exotic particles with masses below $O(10)\text{GeV}/c^2$. The detector is designed to fully reconstruct the exclusive decays of hidden sector particles and to reject the background down to below 0.1 events in the sample of 2×10^{20} POT.

The detector is based on a 50 m long decay volume, housing a $5 \times 10\text{ m}^2$ spectrometer magnet which is sandwiched between tracker stations. To suppress the background from neutrinos interacting in the fiducial volume, the decay volume is maintained under a vacuum since at atmospheric pressure $\sim 10^5$ neutrino interactions are expected for 2×10^{20} POT. The spectrometer is designed to accurately reconstruct the decaying particle's decay vertex, its mass and its impact

¹In the SHiP coordinate system the z -axis is along the beam line and the y -axis is pointing upward.

parameter. Behind the last tracking station, a dedicated timing detector with resolution less than 100 ps measures the coincidence of the decay products, which allows the rejection of combinatorial backgrounds. The timing detector is followed by a set of calorimeters and by muon chambers to provide identification of electrons, photons, muons and charged hadrons. The decay volume is surrounded by background taggers to detect the products of neutrino and muon inelastic scattering in the surrounding structures, which may produce long lived Standard Model V^0 particles, such as K_L , that have a similar decay topology to the expected signals.

The experimental facility is also ideally suited for studying interactions of the least known tau neutrinos [3]. It will therefore host in between the muon shield and the decay volume an emulsion target with a maximum acceptable charged particle flux of $10^3/\text{mm}^2$ for an exposure based on the emulsion cloud concept developed in OPERA [4] and a muon spectrometer.

In the simulation, fixed target collisions of protons are generated by PYTHIA8 [5], neutrino interactions by GENIE [6] and inelastic muon interactions by PYTHIA6 [7]. The heavy flavor production in cascade interactions is also taken into account [8]. The SHiP detector response is simulated in the GEANT4 [9] framework. All the simulation is performed within the FairRoot [10] framework.

While muons can easily be deflected out of the acceptance of the spectrometer by a magnetic field, the problem is the large spread in the phase space of muons, as shown in figure 1, with the consequence that the return field of the magnets tend to bend muons back towards the spectrometer. The DONUT [3] experiment employed a combination of magnetic and passive shielding to clear muons from their emulsion target, which was located 36 m downstream of the target. SHiP will accumulate three orders of magnitude more protons on target, and hence requires a much larger reduction in muon flux for both the emulsion and the hidden sector particles search. To achieve this SHiP will employ the novel magnetic shielding concept described in this paper.

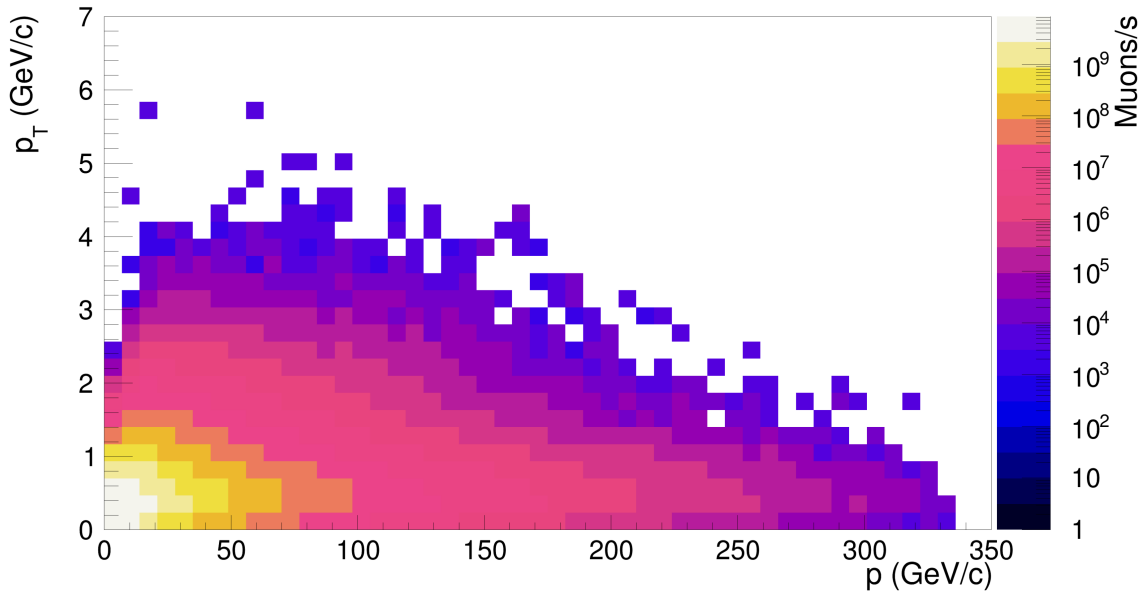


Figure 1. Transverse momentum versus momentum distribution of muons, as generated by Pythia [5, 7].

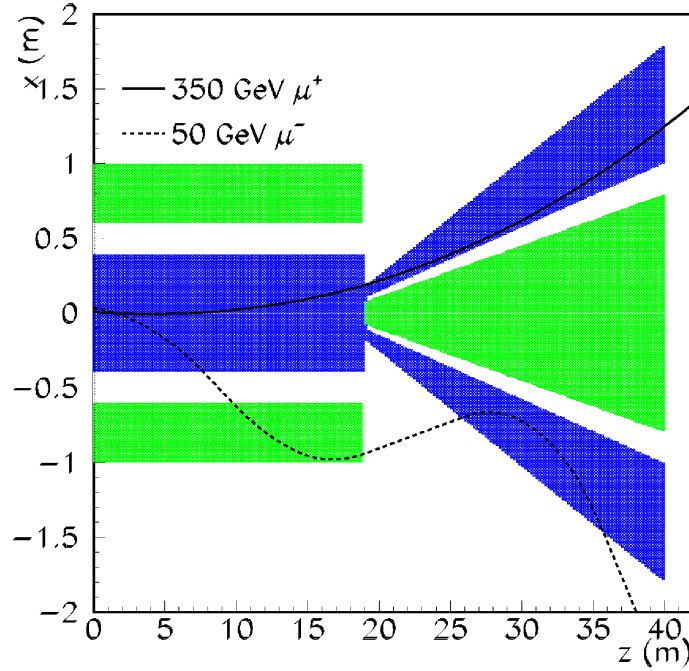


Figure 2. Cross section at $y = 0$ shows the principle of magnetic shielding. The magnetic field is along the y -axis, and its polarity is indicated by the blue/green color of the iron poles of the magnets. The trajectories of a 350 GeV/c muon and 50 GeV/c muon are shown with a full and dashed line, respectively.

The basic magnetic configuration that addresses these issues is presented in the next section. Section 3 describes the optimization procedure with a simplified Monte Carlo tool to obtain a layout which reduces the muon flux sufficiently for a minimum size of the system. The optimization is checked by implementing the obtained layout in the GEANT4-based SHiP software package, and its performance is presented in section 4. The last section discusses possible improvements and gives an outlook for obtaining the final design of the SHiP muon shield.

2 The basic principle of magnet based muon shielding

The principle of the magnet based shielding is shown in 2-D in figure 2. The first part of the shield should be long enough, i.e. providing sufficient $\int Bdl$, to separate both muon polarities to either side of the z -axis. For a 350 GeV/c muon, taking into account the p_T distribution at its production point, this requires a ~ 18 m long magnet with a field² in the iron of 1.8 T.

Lower momentum muons, which traverse the return field of this magnet, will be bent back in the direction of the spectrometer as is shown in figure 2 for a 50 GeV/c muon. To shield the spectrometer from these muons, an additional magnet is added with opposite polarity field close to the z -axis, and hence the lower momentum muons will be swept out again. At the start of this second magnet, the two field polarities should be as close in x as possible. A magnet design study [11]

²When using a high permeability material such as Grain Oriented steel a 1.8 T flux density could be obtained while the coils would dissipate low enough power so that they could be cooled with air [11].

shows that an air gap as small as 2 cm between the two field polarities can be used without distorting the 1.8 T field in the iron.

3 Simulations and optimization

To test the basic principle of the muon shielding concept described in section 2 and optimize its layout, a fast program was written which traces the muons through the magnets. Each magnet is described by the following seven parameters: length and, at either end, widths, heights, and air-gap widths between field and return field. Muons are traced through a setup with a step size of 5 cm, and only the following physics processes are taken into account: bending in a 1.8 T magnetic field, specific energy loss (dE/dx) and Gaussian smeared multiple Coulomb scattering.

The aim is to design the shortest possible shield which allows no muons to reach the spectrometer, while at the same time being affordable and hence using as little iron as possible. These requirements are combined into a single penalty function which is then minimized. The penalty function is given by

$$\frac{W \times (1 + \sum \chi_{\mu^+})}{A} \quad (3.1)$$

where:

- All muons are assigned a positive charge, and the magnetic fields are oriented to bend the muons towards positive x at the last tracking station. The transverse (x, y) position of muons is obtained at the last tracking station, which has a sensitive area of $5 \times 10 \text{ m}^2$, by tracing their trajectory 64 m downstream of the shield. Their position at the last tracking station is converted to a smooth function to allow the optimization to sense that it moves all μ^+ out of the acceptance of the last tracking station. Hence, with $|y| < 5 \text{ m}$, their x -position is converted into $\chi_{\mu^+} = \sqrt{(5.6 - (x + 3.))/5.6}$ for $-3 < x < 2.6 \text{ m}$, else $\chi_{\mu^+} = 0$;
- $A = 1. - L/100$: approximately the relative acceptance of a new long lived particle in a benchmark scenario, where L is the length of the shield in m;
- W : weight of the shield in tonnes of iron;
- The sum is taken over all muons.

The optimization uses Minuit [12] to minimize penalty function (3.1) by varying the size of the magnets. Only muons with $p(\mu) > 1 \text{ GeV}/c$ at the last tracking station are considered as background muons, since only larger momentum tracks will be used in the searches. Magnet transverse sizes are only allowed to vary by quanta of 1 cm. Magnet length sizes are only allowed to vary by quanta of 10 cm. To assure that a muon which traverses the same geometry returns the same contribution to the penalty function the tracing of each muon is always started with a random number seeded by its momentum. For simplicity, the optimization is made with seven magnets. Future work will try to vary the number of magnets. The first two magnets after the beam dump are also required for radiation protection and their lengths are fixed to 1.4 and 3.4 m respectively, their gaps are fixed to 2 cm and they have the same height at either end of each magnet.

Muons have been generated with Pythia [5, 7], corresponding to $\sim 10^{10}$ POT, and the Minuit SIMPLEX function varies 41 parameters to minimize the penalty function. After convergence,

none of the muons traverse the last tracking station for a total shield length of 34 m. Its layout and performance is presented in the next section.

4 Active muon shield performance

The SHiP experiment simulations are performed in the software package FairShip [1]. FairShip is mostly a collection of libraries and scripts based on the FairRoot framework [10], which is fully based on the ROOT software framework [13]. In the framework, users can construct their detectors, and perform simulation and analysis without any code dependence on a specific Monte Carlo simulation software. FairRoot uses the ROOT geometry package TGeo to build, browse, track and visualize a detector geometry. The muon shield can be made of two different magnet types, that are depicted in figure 3. When there is enough air-gap between the iron yokes with the opposite field direction to place a coil a magnet of type a) in figure 3 is used. If the optimization requires an air-gap which is too small to accommodate a coil, a magnet of type b) in figure 3, which has place for coils at the top and bottom, is used.

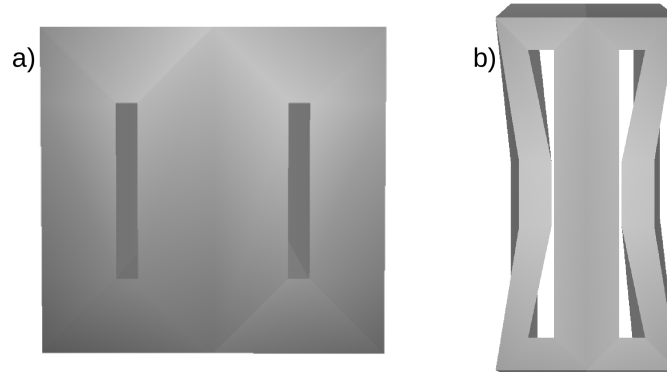


Figure 3. A view in the x - y plane of the two magnet configurations. In configuration a) the air-gap is large enough anywhere along y to place a coil. Configuration b) has an air-gap close to 2 cm at $y = 0$, and hence the program will create large enough air-gaps at the top and bottom of the magnet to accommodate the coils.

In addition, the following boundary conditions are imposed to assure a realistic implementation of the magnets:

- For every cross section in the xy -plane, the width of the iron is large enough everywhere to sustain the same magnetic flux;
- Minimum air-gap between opposite field directions is 2 cm;
- Minimum air-gap for accommodating coils in the plane perpendicular to the beam direction is 20 cm;
- Minimum air-gap between magnets along the beam direction is 10 cm;
- Mitred joints between volumes with horizontal and vertical fields are imposed to lower their magnetic reluctance [11].

The geometry optimization results in a shield layout shown in figure 4, weighing 1845 tonnes, which does not include the supports.

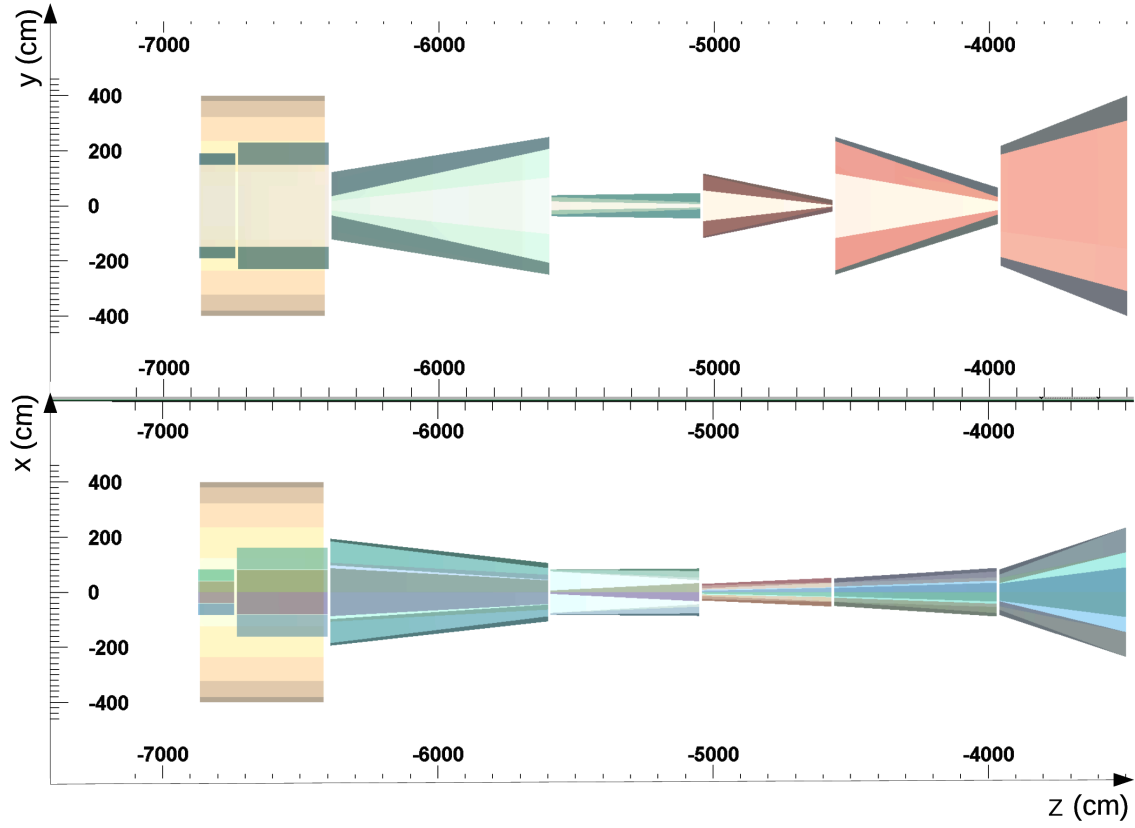


Figure 4. Geometric view of the optimized muon shield, showing at the top, the z - y plane view, and at the bottom, the z - x plane view. SHiP defines the origin of the coordinate system to be in the center of the decay vessel. Color shading is used to enhance the contrast between different magnetic field orientations.

To test the background with the prototype shielding in FairShip, only target, muon shield, tracking stations and spectrometer magnet were included in the simulation. The last tracking station is located 64 m downstream of the last shielding magnet.

The simulation is first run with all the material of the shield in place, but with the magnetic field switched off. This results in $\sim 3.1 \times 10^9$ muons which traverse the last tracking station during one SPS spill of 4×10^{13} POT. Switching on the magnetic field reduces this rate to $\sim 3.0 \times 10^5$ muons/s, of which $\sim 6.5 \times 10^4$ have momenta larger than 3 GeV/c. These muon rates are sufficiently low to cause insignificant background levels in the experiment.

Examining the muons which do reach the last tracking station reveals that they are mainly due to two effects which are not included in the optimization procedure, namely catastrophic energy loss [14] and very large scattering angles.

5 Discussion and outlook

A magnetic deflecting system for muons is presented, which provides the required rate reduction of muons for the SHiP experiment and fulfills the emulsion requirements described in the introduction. The design is optimized to reduce muon background in the spectrometer for the shortest possible shield and the lowest iron usage. The optimized geometry of the shield is 34 m long and its weight is 1845 tonnes not including its supports. As coming from FairShip simulation, given that the muons which do traverse the system are due to physics processes which have not been included in the optimization program, the shield will be further optimized using all physics processes as implemented in GEANT4 [9]. This will increase the required CPU time by several orders of magnitude. In addition, it is found that a large flux of electrons and photons is produced by the muons traversing the magnets. Their momentum is typically below a GeV/c, and hence they do not constitute a source of background directly. However, the SHiP decay vessel is surrounded by detectors to tag any charged particle entering the vessel. Moreover, the emulsion target upstream is also sensitive to low energy electrons that may spoil its reconstruction capability. Hence, the flux of these particles has to also be controlled to ensure an effective use of these surround taggers. A future optimization will include the flux of electrons and photons through the taggers and emulsion detectors in the penalty function.

References

- [1] SHiP collaboration, M. Anelli et al., *A facility to Search for Hidden Particles (SHiP) at the CERN SPS*, [arXiv:1504.04956](#).
- [2] S. Alekhin et. al, *A facility to Search for Hidden Particles at the CERN SPS: the SHiP physics case*, *Rep. Prog. Phys.* **79** (2016) 124201.
- [3] DONUT collaboration, K. Kodama et al., *Observation of tau neutrino interactions*, *Phys. Lett. B* **504** (2001) 218 [[hep-ex/0012035](#)];
DONuT collaboration, K. Kodama et al., *Final tau-neutrino results from the DONuT experiment*, *Phys. Rev. D* **78** (2008) 052002 [[arXiv:0711.0728](#)].
- [4] R. Acquafredda et al., *The OPERA experiment in the CERN to Gran Sasso neutrino beam*, 2009 *JINST* **4** P04018.
- [5] T. Sjöstrand, S. Mrenna and P.Z. Skands, *A Brief Introduction to PYTHIA 8.1*, *Comput. Phys. Commun.* **178** (2008) 852 [[arXiv:0710.3820](#)].
- [6] C. Andreopoulos et al., *The GENIE Neutrino Monte Carlo Generator*, *Nucl. Instrum. Meth. A* **614** (2010) 87 [[arXiv:0905.2517](#)].
- [7] T. Sjöstrand, S. Mrenna and P.Z. Skands, *PYTHIA 6.4 Physics and Manual*, *JHEP* **05** (2006) 026 [[hep-ph/0603175](#)].
- [8] H. Dijkstra and T. Ruf, *Heavy Flavour Cascade Production in a Beam Dump*, *SHiP-NOTE-2015-009* (2015).
- [9] GEANT4 collaboration, S. Agostinelli et al., *GEANT4: A Simulation toolkit*, *Nucl. Instrum. Meth. A* **506** (2003) 250.
- [10] MM. Al-Turany, D. Bertini, R. Karabowicz, D. Kresan, P. Malzacher, T. Stockmanns et al., *The FairRoot framework*, *J. Phys. Conf. Ser.* **396** (2012) 022001.

- [11] V. Bayliss, M. Courthold and T. Rawlings, *Active Muon Shield — Preliminary Design Report*, [CERN-SHiP-NOTE-2015-003](#) (2015).
- [12] F. James, *MINUIT Function Minimization and Error Analysis: Reference Manual Version 94.1*, CERN Program Library Long Writeup D506 (1998).
- [13] R. Brun and F. Rademakers, *ROOT: An object oriented data analysis framework*, [Nucl. Instrum. Meth. A 389](#) (1997) 81.
- [14] K. Bachas et al., *Studies of catastrophic muon energy losses in ATLAS H8 combined Testbeam data*, *Nucl. Phys. (Proc. Suppl.) B 177-178* (2008) 320.